Available online at www.sciencedirect.com

SciVerse ScienceDirect

Ceramics International 39 (2013) 1711–1716

CERAMICS INTERNATIONAL

www.elsevier.com/locate/ceramint

Effect of V_2O_5 doping on microstructure and electrical properties of Bi_2O_3–TiO_2 solid oxide electrolyte system

Chun-Ming Lin*, Yu-Lin Kuo, Chia-Hao Chou

Department of Mechanical Engineering, National Taiwan University of Science and Technology, Taipei 10673, Taiwan

Received 30 June 2012; received in revised form 20 July 2012; accepted 8 August 2012
Available online 18 August 2012

Abstract

V_2O_5 in the Bi_2O_3–TiO_2 system (14BTO) is used as an electrolyte material for solid oxide fuel cell (SOFC) applications. Material characterization and electrical behavior of 10VO, and 25VO, 50VO molar (mol) ratio doped 14BTO specimens were investigated by X-ray diffraction (XRD), field emission scanning electron microscopy (FE-SEM) and two-probe DC conductivity measurement method. The XRD results show that cubic sillenite single phase ($Bi_{12}TiO_{20}$) is observed in the 14BTO-10VO and 14BTO-25VO specimens and two phases ($Bi_{12}TiO_{20}$ and $Bi_4V_{15}Ti_{0.5}O_{10.85}$) in the 14BTO-50VO specimen. In situ and batch-type long-term conductivity measurements at 600 °C were conducted to verify the possible reason of degradation which may have occurred in the 14BTO samples in this study.

Keywords: Mixing; Porosity; Electrical conductivity; Batteries

1. Introduction

Solid oxide fuel cells (SOFCs) are highly efficient producers of electricity, through the direct oxidization of fuels. Thermodynamic analysis of an SOFC system based on an oxygen ion conductor has shown that the maximum efficiency varies from 68 to 82 within a temperature range of 600–1000 °C [1]. Bi_2O_3 has a -cubic composition, which contributes to its exceptional ionic conductivity of oxygen ions. This material has been extensively investigated through computer simulations and experimental analyses in order to assess its suitability for SOFC electrolyte applications. The problems associated with using Bi_2O_3 as an SOFC electrolyte include low chemical stability in reduction atmospheres and phase stability within a limited temperature range. It has been reported that Bi_2O_3 becomes unstable when the partial pressure of oxygen is below 10^{-6} Pa at 700 °C [2]. Thus, an additional barrier layer is required to prevent the surface of the Bi_2O_3-based electrolyte from being reduced. Suitable doping can stabilize the high ionic conduction phase at a broader working range, which includes lower temperatures [2–5]. A number of oxides have been shown to possess an acceptable level of photonic conductivity [6]. These oxides are applicable as electrolytes in an SOFC. However, since atmosphere at elevated temperatures is not stable in oxides (i.e., BaCeO, SrCeO and CaZrO), it is not suitable for practical applications. SOFCs can be used with a wider range of fuels than other types of fuel cells [7–9] because they operate at relatively high temperatures [10]. This study proposes an SOFC using V_2O_5-doped Bi_2O_3–TiO_2 ($Bi_{12}TiO_{20}$, 14BTO) to compensate for the poor conductivity of Bi_2O_3–TiO_2.

This study focused entirely on the preparation and characterization of V_2O_5-doped 14BTO at various concentrations. In accordance with our previous work [10,11], we employed colloidal processing followed by pressure filtration to obtain specimens of higher quality. X-ray diffraction (XRD, RIGAKU RTP 300) and field emission scanning electron microscopy (FE-SEM, JEOL JSM-6390 LV) were used to examine the microstructural morphology, crystal structure, and surface porosity of the sintered

*Corresponding author. Tel.: +886 2 2737 3141x7304; fax: +886 2 2737 6460.
E-mail address: D9503503@mail.ntust.edu.tw, clin112@asu.edu (C.-M. Lin).

0272-8842/$ - see front matter © 2012 Elsevier Ltd and Techna Group S.r.l. All rights reserved.
http://dx.doi.org/10.1016/j.ceramint.2012.08.015

pellets. The Archimedes method was applied to measure the relative density of the samples. In-situ and batch-type long-term conductivity measurements were carried out at 600 °C for as long as 24 h to investigate the reasons for degradation.

2. Experimental procedures

2.1. Material preparation

Bi_2O_3 powder (99.9, Solartech, Taiwan), TiO_2 powder (99.9, Alfa Aesar, USA) and V_2O_5 powder (99.9, Merck, KGaA, Darmstadt) were used to prepare V_2O_5-doped Bi_2O_3-TiO_2 specimens by colloidal process-pressure filtration. The purchased TiO_2, Bi_2O_3 and V_2O_5 powders were separately dispersed in de-ionized water with 1 wt (according to oxide powder) of D-134 dispersant (ammonium salt homopolymer with a 2-propenoic acid group; Dai-Ichi Kogyo Seiyaku Co. Ltd., Japan) and then ball-milled for 24 h to ensure well-mixed slurries.

2.2. Material characterization

The powders were verified by XRD to be monoclinic Bi_2O_3 and tetragonal anatase TiO_2. Characterization of powders was investigated using an FE-SEM. Stoichiometric 14.3 mol of titania slurry was then added into the Bi_2O_3 slurry for another 2 h of ball-mill mixing, forming Bi_2O_3–TiO_2. Following the same method, stoichiometric 28.3 mol of V_2O_5 slurry was added in various molar ratios into Bi_2O_3–TiO_2 slurry and ball-milled for another 2 h; the slurry was then pressure filtrated in a self-designed acrylic mold at 10 atm. This was followed by sintering of the green disks for 2 h at 850 °C with a heating rate of 10 °C min^{-1}. For comparison, 14BTO powder was also prepared by die-pressing at 140 MPa. The exact crystal phases of the materials were obtained by XRD. The incident beam was Cu K characteristic X-ray at 40 kV and 100 mA. Secondary electron images (i.e., SEI image) from FE-SEM revealed the microstructural morphology of the specimens. The densities of the sintered 14BTO disks were derived by Archimedes relation. Conductivities of the specimens were measured at temperatures ranging from 500 to 700 °C. Platinum electrodes of 0.1 cm diameter were secured to either sides of the sample pellet using Heraeus CL11-5100 Pt adhesive paste and held at high temperature for 1 h. Two-probe DC conductivity was measured. Long-term conductivity measurements at 600 °C by in situ and batch-type methods were conducted to verify the possible reason of degradation of 14BTO samples. In situ long-term conductivity measurement was continuously recorded for 24 h. Aging test was performed for 14BTO samples placed in a furnace with an aging temperature of 600 °C for the batch-type long-term conductivity measurement, and each sample was removed from the furnace at a specific time for further conductivity measurements.

3. Results and discussion

3.1. X-ray diffraction analysis

Specimens sintered at a temperature of 850 °C were examined by XRD after the pressure filtration process as shown in Fig. 1. All the specimens revealed a single phase $Bi_{12}TiO_{20}$ with a cubic sillenite structure, and the strongest diffraction peak of the (310) plane was at a 2θ of 27.7° (note that the structure had the smallest mismatch in peak location). Furthermore, for 14BTO doped with 10, 25 and 50 mol V_2O_5 (hereafter, 14BTO-10VO, 14BTO-25VO, and 14BTO-50VO, respectively) and treated at 850 °C for 2 h, the peaks shifted slightly towards right from about 27.7° to 27.8°. In particular, the structure of a single crystal doped with 10 M ratios of V_2O_5 (i.e., 14BTO-10VO) remained unchanged. An increase in the molar (mol) ratio beyond 25 (i.e., 14BTO-25VO) resulted in a significant shift in the peak position. The $Bi_{12}TiO_{20}$ and $Bi_4V_{15}Ti_{0.5}O_{10.85}$ phases coexisted in 14BTO-50VO specimens. An increase in V_2O_5 molar ratios also reduced the peaks.

As discussed above, the strongest peak shifted to a lower diffraction angle, implying that the increased lattice constant of 14BTO was correlated with an increase in the molar ratio of V_2O_5. The calculated lattice constants for each case are shown in Fig. 2. Compared with the lattice constant of 10.164 Å from the single crystal $Bi_{12}TiO_{20}$, the sintered 14BTO specimens showed a larger lattice parameter (i.e., 10.164 Å), which decreased with the molar ratio of V_2O_5: from 10.175 Å for 10VO, to 10.144 Å for 50VO. Defect concentration is associated with a change in molar ratio. Thus, the variation in lattice constants is an indicator of the concentration of defects in the crystal structure. V_2O_5 is well known to cause intrinsic defects at increased molar ratios. It is possible that the number of structural defects in $Bi_{12}TiO_{20}$ may also increase at higher temperatures. A higher concentration of lattice defects locally distorts the lattice structure, which leads to an expansion of the average lattice parameter following an

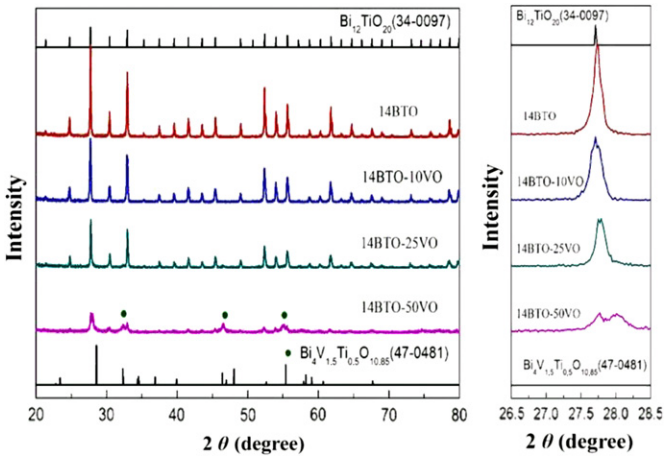

Fig. 1. XRD spectra of 14BTO, and 14BTO-10VO, 14BTO-25VO and 14BTO-50VO specimens.

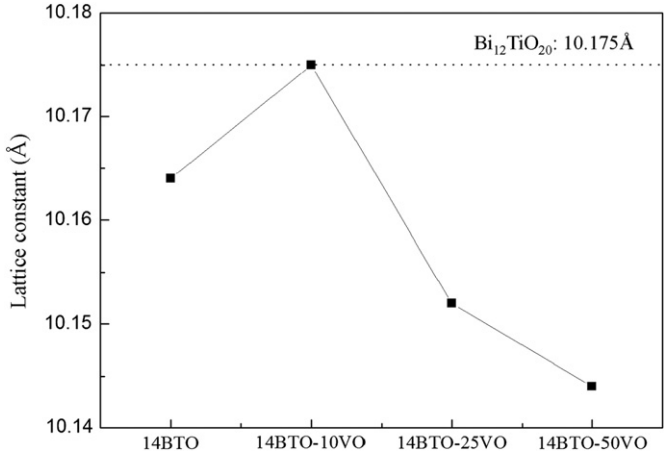

Fig. 2. Lattice constants of 14BTO as a function of V_2O_5 dope concentration.

increase in molar ratio. This would explain the variation in the peak position of the four separately sintered specimens.

In addition, the densities of the sintered specimens measured using the Archimedes method (AM) showed various molar ratios of V_2O_5, which can be inferred from the porosity of the 850 °C sintered specimens, corresponding to a high sintered density for all doped conditions. The densities of the specimens were separately measured using AM. The relative densities of the 14BTO, 14BTO-10VO, 14BTO-25VO, and 14BTO-50VO specimens sintered at 850 °C were 54.50, 67.98, 94.96, and 96.82, respectively. Comparing with the die-pressed specimens, the highest sintered density is 96.82 under 850 °C for 2 h of heat treatment, which is lower than that for the case by pressure filtration [10,12]. This result is similar to that previously reported on the basis of the investigation on densities of die-pressed and pressure-filtration sintered mixed powders. Therefore, it has been shown that pressure filtration results in relatively higher sintered densities with a more uniform packing property.

3.2. Microstructural and sintered density analysis

Microstructure (i.e., SEM images) examination indicated that the application of a ball-mill narrowed the distribution to 2.2, 0.5, and 1.6 m for Bi_2O_3, TiO_2, and V_2O_5, respectively. (Note that the average diameters of the starting powders were 2–3 m for Bi_2O_3, in the sub-micron limit for TiO_2, and 1–2 m for V_2O_5.) In addition, plane view and cross-sectional SEM images (i.e., secondary electron images (SEI image)) of the sintered specimens are shown in Fig. 3. The porosity derived from AM was 6.24 at a bulk density of 8.346 g/cm^3, while that from the SEI image was calculated to be 14.40. It is also evident that the porosity of sample sintered at 850 °C corresponded well with the high sintered density obtained by AM (see Table 1). In addition, the microstructure of the polished surfaces of sintered 14BTO, 14BTO-10VO, 14BTO-25VO, and 14BTO-50VO specimens were observed. For 14BTO specimens, a homogeneous solid solution was confirmed by SEI mode. For 14BTO-10VO and 14BTO-25VO specimens, the existence of single phase microstructure can be observed in the SEM images; the grey area in the figure is the $Bi_{12}TiO_{20}$ matrix. However, porosity was significantly increased between the 14BTO-10VO and the 14BTO-25VO specimens (i.e., 14BTO-25VO significantly increased compared with that of 14BTO-10VO). Finally, in the 14BTO-50VO specimen, the tendency towards an increase in porosity with V_2O_5 molar (mol) ratio was also evident in the SEM image, due to the existence of a two-phase microstructure., The white particles in the figure represent $Bi_4V_{15}Ti_{0.5}O_{10.85}$, and the grey area represents the $Bi_{12}TiO_{20}$ matrix. These microstructural changes within the V_2O_5-doped 14BTO may be indicative of a suitable SOFC electrolytic material, as we see a good microstructural morphology and high sintered density for the 50VO molar dope conditions.

3.3. Electrical properties

Fig. 4 shows the Arrhenius plot of the conductivities of 14BTO-10VO, 14BTO-25VO and 14BTO-50VO specimens determined by the two-probe DC conductivity measurement method. Bulk YSZ, Bi_2O_3 and 14BTO specimens were also measured for comparison [10]. The conductivity of 14BTO specimen is lower than that of the common SOFC electrolyte material, i.e., YSZ, which has a few orders higher conductivity. But conductivity of 14BTO specimen is higher than that of Bi_2O_3. A one-step conductivity feature of the 14BTO specimen represents a stable phase without any phase transition as observed in Bi_2O_3. However, the conductivities of 14BTO-10VO and 14BTO-25VO specimens are higher than that of the 14BTO specimen. A further doping to 50VO molar (mol) ratio in 14BTO causes an increase in the conductivity to higher than that of YSZ. Due to the sillenitic crystalline structure of the $Bi_4V_{15}Ti_{0.5}O_{10.85}$, tetrahedrally coordinated Ti^{4+} cations occupy the bcc sites while the Bi^{3+} assume the hepta-coordinated positions. However, an increase in the V_2O_5 molar (mol) ratio increases the likelihood that the bcc sites will be occupied, due to the octahedrally coordinated V^{5+} transfer to V^{4+} (i.e., under high temperature conditions) [13]. The atom positions are relatively fixed compared with that of conducting ionic Bi_2O_3. Oxygen anions are considered to exhibit mobility. In a study of similarly structured Bi_2O_3 based sillenites, those that have lattice structures are seen to exhibit the lowest conductivity values [10,14]. By contrast, $Bi_4V_{15}Ti_{0.5}O_{10.85}$ sillenites increased to a doped molar (mol) ratio of 50VO in 14BTO, due to the presence of inner defects. Note that at higher temperatures, this involved the misplacement of titanium or vanadium cations by titanium-vacancy complex, vanadium-vacancy complex, or bismuth cations at bcc sites [15,16]. The misplaced bismuth cations induce charge imbalance, suggesting that electron–holes pair with bismuth cations at vanadium cation sites.

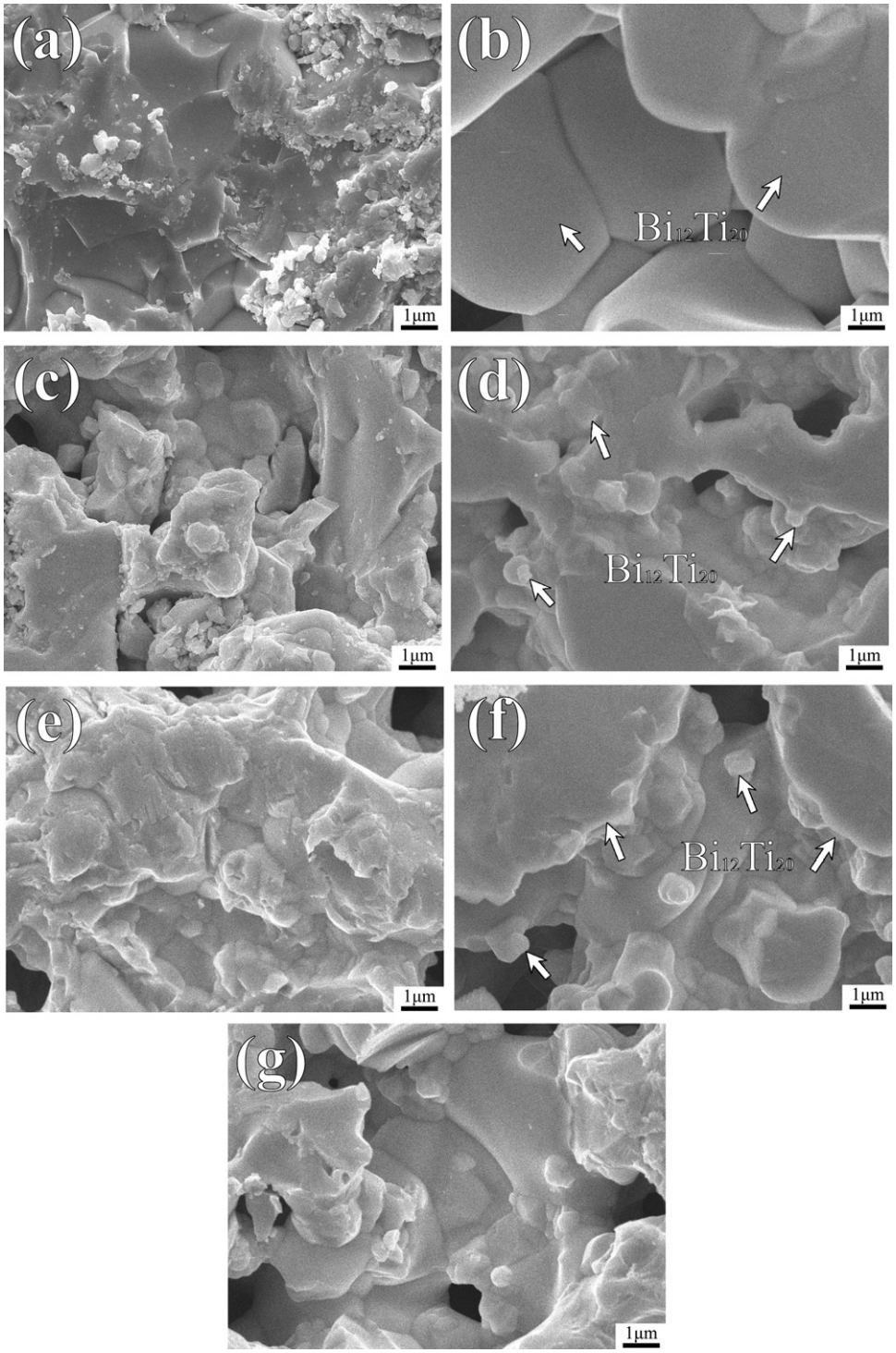

Fig. 3. SEM surface morphology of (a) 14BTO, (c) 14BTO-10VO, (e) 14BTO-25VO, (g) 14BTO-50VO specimens sintered at 850 °C for 2 h, and cross-sectional microstructures of sintered (b) 14BTO, (d) 14BTO-10VO, (f) 14BTO-25VO and (h) 14BTO-50VO specimens.

The defect–hole pair would result in an n-type electronic conduction. In experimental analyses of [17,18], the activation energy (Ea) of 0.99 eV, closely corresponding to the activation energy of semiconductors, is lower than that of the 14BTO-50VO specimen sintered at 850 °C in this study (Ea = 1.46 eV). However, the conductivity of $Bi_4V_{15}Ti_{0.5}O_{10.85}$ is higher than that of our specimens (see Table 2) in the temperature range of 400–700 °C, which could be due to mixed conduction because of increased oxygen vacancies [13,19].

In addition to the thermal stability test, many studies that assess $Bi_4V_{15}Ti_{0.5}O_{10.85}$ electrolytes seek long-term stability. For this, the 14BTO-50VO specimen was held at 600 °C and in situ two-probe DC conductivity was measured up to 24 h, as shown in Fig. 5. The conductivity was found to decrease drastically within the initial 6 h (i.e.,

prolonged heating past 6 h resulted in 3.5×10^{-3} S/cm); in contrast, the conductivity decreased with an increase in heating time. As discussed above, the possible reasons of conductivity degradation occurred in the phase separation or defect ordering processes. In [20,21], it was reported that the radical drop in conductivity in the first 6 h is characteristic of these structures. In that study of RE_2O_3–Bi_2O_3 systems, structural ordering was the result of face centered cubic (fcc)–rhombohedral transformation, which resulted in lower conductivity [10,17]. In addition, because no structural changes were observed throughout the course of conductivity decay [10,11,20–23], the properties may have underwent a form of ordering or relaxation, which can be reversed at the order–disorder transition temperature. Beginning with highly disordered fcc based bismuth oxides, the transition behavior may be best represented by cation ordering and anion or vacancy ordering. Cation ordering was proposed due to elastic diffuse neutron scattering. The Yb_3 cations may be restricted to the corners of the cubes, reducing the symmetry of the bismuth fcc lattice. In addition, in classical mechanic simulations, the polarizability of oxygen has been shown to have no effect on diffusion [13]. This means that the ordering of fewer polar dopant cations could have a greater influence on the immobility of oxygen anions than on the ordering of oxygen anions. However, in long term annealing, the ordering of oxygen vacancies will occur.

Table 1
Properties of V_2O_5 doped 14BTO sintered at 850 °C for 2 h.

Conditions of sintering	Shrinkage (%)	Bulk density (g/cm^3)	Porosity (%)	Relative density (%)
14BTO	34.10	8.35	7.99	96.82
14BTO-10VO	−15.24	4.68	49.43	54.50
14BTO-25VO	−4.66	5.65	35.53	67.98
14BTO-50VO	43.09	7.93	6.24	94.96

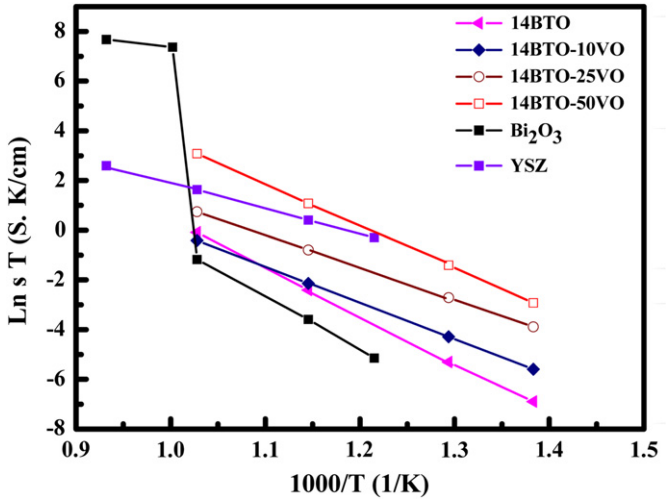

Fig. 4. Arrhenius plot of conductivity as a function of temperature for 14BTO, 14BTO-10VO, 14BTO-25VO and 14BTO-50VO specimens, as well as bulk Bi_2O_3 and YSZ.

4. Conclusions

The present experimental results have shown that the 14BTO-10VO, 14BTO-25VO, and 14BTO-50VO specimens (note that 14BTO-10VO and 14BTO-25VO have a sillenite single phase and 14BTO-50VO has two phases) were prepared through a suitable colloidal process followed by the pressure filtration method and subsequently sintered at 850 °C for 2 h. A number of studies have shown that 14BTO-50VO ($Bi_{12}TiO_{20}$ and $Bi_4V_{15}Ti_{0.5}O_{10.85}$) is associated with high relative sintered density and improved conductivity. Thus, control of the solid state electrolyte formation process by manipulating solidification processing variables such as the composition (molar ratio), sintering temperature and time can be applied as an alternative method to produce components that achieve optimal properties.

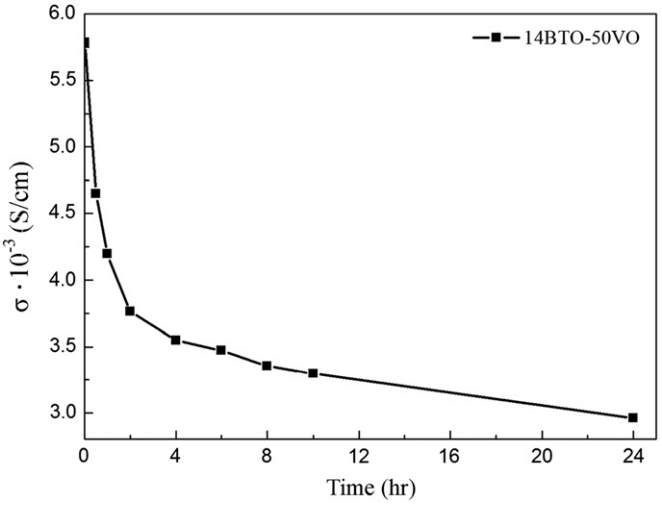

Fig. 5. Variation of total conductivity of 14BTO samples measured at 600 °C as a function of time.

Table 2
Total conductivities and activation energies of V_2O_5-doped 14BTO electrolytes.

	σ_{700}	σ_{600}	σ_{500}	σ_{450}	σ_{400}	Ea (eV)
14BTO	9.13×10^{-4}	8.70×10^{-5}	7.62×10^{-6}	1.41×10^{-6}	2.21×10^{-7}	1.62
14BTO-10VO	6.73×10^{-4}	1.37×10^{-4}	1.83×10^{-5}	5.05×10^{-6}	1.22×10^{-6}	1.26
14BTO-25VO	2.06×10^{-3}	5.48×10^{-4}	9.11×10^{-5}	2.67×10^{-5}	7.92×10^{-6}	1.12
14BTO-50VO	2.08×10^{-2}	3.71×10^{-3}	3.49×10^{-4}	6.68×10^{-5}	1.46×10^{-5}	1.46

References

[1] A.K. Demin, V. Alderucci, I. Ielo, G.I. Fadeev, G. Maggio, N. Giordano, V. Antonucci, Thermodynamic analysis of methane fueled solid oxide fuel cell system, International Journal of Hydrogen Energy 17 (6) (1992) 451–458.

[2] P. Shuk, H.-D. Wiemhofer, U. Guth, W. Gopel, M. Greenblatt, Oxide ion conducting solid electrolytes based on Bi_2O_3, Solid State Ionics 89 (1996) 179–196.

[3] K. Laurent, G.Y. Wang, S. Tusseau-Nenez, Y.L. Wang, Structure and conductivity studies of electrodeposited -Bi_2O_3, Solid State Ionics 178 (2008) 1735–1739.

[4] N. Jiang, E.D. Waschman, Structural stability and conductivity of phase-stabilized cubic bismuth oxides, Journal of the American Ceramic Society 82 (1999) 3057–3064.

[5] N.M. Sammes, G.A. Tompsett, H. Nafe, F. Aldinger, Bismuth based oxide and ionic conductivity, Journal of the European Ceramic Society 19 (1999) 1801–1826.

[6] K. Katahira, Y. Kohchi, T. Shimura, H. Iwahara, Protonic conduction in Zr-substituted BaCeO3, Solid State Ionics 138 (2000) 91–98.

[7] A. Demin, P. Tsiakara, Thermodynamic analysis of a hydrogen fed solid oxide fuel cell based on a proton conductor, International Journal of Hydrogen Energy 26 (10) (2001) 1103–1108.

[8] A.K. Demin, P.E. Tsiakaras, V.A. Sobyanin, S.Y. Hramova, Thermodynamic analysis of a methane fed SOFC system based on a protonic conductor, Solid State Ionics 152–153 (2002) 555–560.

[9] M. Ihara, K. Matsuda, H. Sato, C. Yokoyama, Solid state fuel storage and utilization through reversible carbon deposition on an SOFC anode, Solid State Ionics 175 (1–4) (2004) 51–54.

[10] Y.L. Kuo, L.D. Liu, S.E. Lin, C.H. Chou, J.W.C. Wei, Assessment of structurally stable cubic $Bi_{12}TiO_{20}$ as intermediate temperature solid oxide fuels electrolyte, Journal of the European Ceramic Society 31 (3) (2011) 3119–3125.

[11] Y.L. Kuo, C. Lee, Y.S. Chen, H. Liang, Gadolinia-doped ceria films deposited by RF reactive magnetron sputtering, Solid State Ionics 180 (2009) 1421–1428.

[12] S. Tekeli, U. Demir, Colloidal processing, sintering and static grain growth behaviour of alumina-doped cubic zirconia, Ceramics International 31 (2005) 973–980.

[13] M. Benmoussa, E. Ibnouelghazi, A. Bennouna, E.L. Ameziane, Structural, electrical and optical properties of sputtered vanadium pentoxide thin films, Thin Solid Films 265 (1–2) (1995) 22–28.

[14] J.A. Kilner, J. Drennan, P. Dennis, B.C.H. Steele, A study of anion transport in bismuth based oxide systems by electrical conductivity and secondary ion mass spectroscopy (SIMS), Solid State Ionics 5 (1981) 527–530.

[15] R. Oberschmid, Absorption centers of $Bi_{12}GeO_{20}$ and $Bi_{12}SiO_{20}$ crystals, Physica Status Solidi A 89 (1985) 263–270.

[16] J.F. Carvalho, F.R.W. Aranco, C.J. Magon, L.A.O. Nunes, Vanadium characterization in BTO: V sillenite crystals, Materials Research 2 (1999) 89–91.

[17] S. Lanfredi, M.A.L. Nobre, Conductivity mechanism analysis at high temperature in bismuth titanate: a single crystal with sillenite-type structure, Applied Physics Letters 86 (2005) 1–3.

[18] S. Lanfredi, J.F. Carvalho, A.C. Hernandes, Electric and dielectric properties of $Bi_{12}TiO_{20}$ single crystals, Journal of Applied Physics 88 (2000) 283–287.

[19] C. Sanchez, R. Morineau, J. Livage, Electrical conductivity of amorphous V_2O_5, Physica Status Solidi A 76 (1983) 661–666.

[20] N. Jiang, E.D. Waschman, Structural stability and conductivity of phase-stabilized cubic bismuth oxides, Journal of the American Ceramic Society 82 (1999) 3057–3064.

[21] D. Waschman, S. Boyapati, N. Jiang, New Li^+ ion conductors in the system Li_4SiO_4–Li_3AsO_4, Ionics 7 (2001) 1–8.

[22] K.Z. Fung, J.A.V. Virkar, Phase stability, phase transformation kinetics, and conductivity of Y_2O_3–Bi_2O_3 solid electrolytes containing aliovalent dopants, American Ceramic Society 74 (1991) 1970–1980.

[23] P.D. Battle, C.R.A. Catlow, L.M. Moroney, Structural and dynamical studies of -Bi_2O_3 oxide-ion conductors: II. A structural comparison of $(Bi_2O_3)1-x(M_2O_3)x$ for M = Y, Er, and Yb, Journal of Solid State Chemistry 67 (1987) 42–50.